COMMUNICATIONS IN COMPUTATIONAL PHYSICS
Vol. **4**, No. 3, pp. 611-623

Commun. Comput. Phys.
September 2008

Investigation of Compressible Electromagnetic Flute Mode Instability in Finite Beta Plasma in Support of Z-pinch and Laboratory Astrophysics Experiments

V. I. Sotnikov[1,*], V. V. Ivanov[1], R. Presura[1], J. N. Leboeuf[2], O. G. Onishchenko[3], B. V. Oliver[4], B. Jones[4], T. A. Mehlhorn[4] and C. Deeney[5]

[1] *University of Nevada at Reno, NV 89523, USA.*
[2] *JNL Scientific, Casa Grande, AZ 85222, USA.*
[3] *Institute of Physics of Earth, 123995 Moscow, Russia.*
[4] *Sandia National Laboratories, NM 87123, USA.*
[5] *Department of Energy, Washington, DC 20585, USA.*

Received 7 November 2007; Accepted (in revised version) 12 March 2008

Available online 17 April 2008

Abstract. Flute mode turbulence plays an important role in numerous applications, such as tokamak, Z-pinch, space and astrophysical plasmas. In a low beta plasma flute oscillations are electrostatic and in the nonlinear stage they produce large scale density structures co-mingling with short scale oscillations. Large scale structures are responsible for the enhanced transport across the magnetic field and appearance of short scales leads to ion heating, associated with the ion viscosity. In the present paper nonlinear equations which describe the nonlinear evolution of the flute modes treated as compressible electromagnetic oscillations in a finite beta inhomogeneous plasma with nonuniform magnetic field are derived and solved numerically. For this purpose the 2D numerical code FLUTE was developed. Numerical results show that even in a finite beta plasma flute mode instability can develop along with formation of large scale structures co-existing with short scale perturbations in the nonlinear stage.

AMS subject classifications: 70K75, 82D10, 76F35

Key words: Flute instability, plasma turbulence, nonlinear cascades.

1 Introduction

In the flute or interchange instability the perturbations are uniform parallel to the magnetic field. In cylindrical geometry, the structure resembles a fluted column. In the

*Corresponding author. *Email addresses:* Sotnikov@unr.edu (V. I. Sotnikov), Ivanov@unr.edu (V. V. Ivanov), Presura@unr.edu (R. Presura), jnlscientific@hotmail.com (J. N. Leboeuf), onish@ifz.ru (O. G. Onishchenko), bvolive@sandia.gov (B. V. Oliver), bmjones@sandia.gov (B. Jones), tamehlh@sandia.gov (T. A. Mehlhorn), Chris.Deeney@nnsa.doe.gov (C. Deeney)

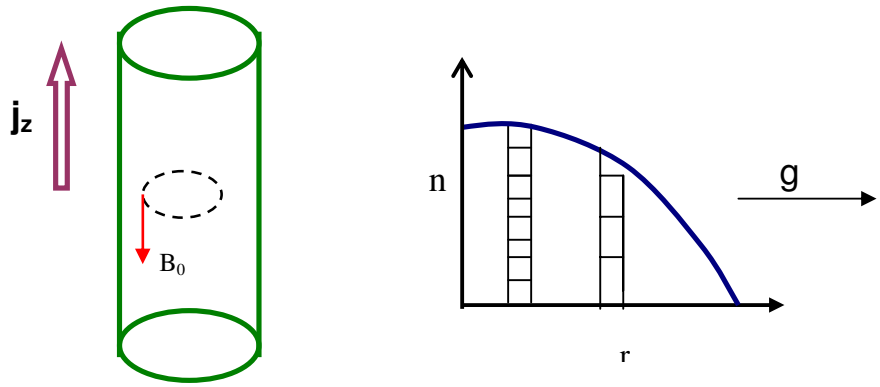

Figure 1: In the left plot the current-carrying plasma in the center of a cylindrical wire array is displayed. In the right plot the radial density dependence inside the plasma cylinder and artificial gravity constant g, associated with the magnetic field lines curvature are presented. A high-density plasma is on top of a low-density plasma in the gravitational field.

current-carrying cylindrical plasma of the precursor (Fig. 1) particles moving along the azimuthal magnetic field lines experience centrifugal acceleration due to the curvature of the magnetic field lines. This acceleration can be explained by introduction of the fictitious gravity force with gravitational constant g, directed outward along the plasma cylinder radius. This configuration creates a situation typical of Rayleigh-Taylor or interchange type instabilities, when a high-density fluid is placed on top of a low-density fluid in a gravitational field. Any perturbation in density at the fluid interface allows gravity to pull the high-density fluid downwards so that the low-density fluid ends up on top. As a result the two fluids interchange places. In plasmas with magnetic fields, both the plasma and the field have pressure and therefore the plasma may interchange position with the magnetic field.

Flute mode turbulence in laboratory and space plasmas can be responsible for formation of large scale structures associated with the anomalous plasma transport across a magnetic field and for appearance of short scales in the turbulent wave spectrum, resulting in enhanced ion heating due to ion viscosity. Analysis of the data obtained during laboratory experiments on imploding wire arrays [1,2] has demonstrated that flute-like perturbations of density appear in the finite beta z-pinch plasma of the precursor. The difference in the electron and ion drifts due to the curvature of magnetic field lines is the source of the flute type instability in the axially current-carrying precursor plasma of cylindrical geometry.

Moreover, density perturbations were observed simultaneously with magnetic field perturbations which were directed along the direction of the ambient magnetic field in the pinch. It was also observed that with time the excited perturbations evolved into large scale structures while the excited wave spectrum migrated into the region of shorter wavelengths.

Laboratory experiments on the interaction of a plasma flow produced by laser ab-

lation of a solid target with the inhomogeneous magnetic field from the Zebra pulsed power generator have also demonstrated the presence of strong wave activity in the region of flow deceleration [3, 4]. Deceleration of the plasma flow can be interpreted as the appearance of a gravity-like force. The drift due to this force can lead to excitation of flute modes. The linear dispersion relation for the excitation of electromagnetic flute-type modes with plasma and magnetic field parameters corresponding to ongoing experiments at the Nevada Terawatt Facility (NTF) has been derived and solved. Results indicate that the wavelength of the excited flute modes strongly depends on the strength of the external magnetic field. For magnetic field strengths <0.1 MG the excited wavelengths are larger than the width of the laser ablated plasma plume and cannot be observed during the experiment. But for magnetic field strengths >0.1 MG the excited wavelengths are much smaller and can then be detected.

Results of these experiments are related to supernova explosions [5], interaction of the solar wind with the magnetopause [6] and active space experiments, such as the artificial magnetospheric releases, similar to the AMPTE magnetotail release [7,8].

2 Two fluid description of compressible flute mode turbulence in a finite beta plasma

Two-fluid macroscopic equations will be used to describe low frequency flute modes [9–11] ($\omega \ll \Omega_i$, where ω is the frequency of the flute mode and $\Omega_i = Z_e B_{0Z}/M_i c$ is the cyclotron frequency of the ion with charge Z and mass $M_i = \mu_a M_p$, M_p being the proton mass and μ_a the atomic weight) in a weakly inhomogeneous plasma with nonuniform external magnetic field $B_{0z}(x)$. As is customary in flute mode turbulence, oscillations are taken to be uniform in the direction of the magnetic field, i.e., the wave vector along the magnetic field $k_{|||} = 0$. We consider a weakly inhomogeneous high beta plasma of slab geometry with density $n_0(x)$ in the presence of an inhomogeneous magnetic field $B_{0z}(x)$, where x is the direction of inhomogeneity. The curvature of the magnetic field lines, consistent with the axial current, causes a centrifugal force on the particles emulated by the gravity-like term $g = g\vec{e}_x$, which drives the instability of the flute modes.

In the high beta precursor plasma of a Z-pinch the electric field in the flute oscillations is not irrotational (i.e., $\nabla \times \vec{E} \neq 0$), as in the low beta case [12–16], and is now written as

$$\vec{E} = -\vec{\nabla}\Phi - \frac{1}{c}\frac{\partial \vec{A}}{\partial t},$$

where Φ and $\vec{A}$ are scalar and vector potentials of the excited wave field. The plasma density N can be expressed as the sum of a slowly varying component with x, the equilibrium plasma density $n_0(x)$, and a perturbed component due to flute oscillations $\delta n(x,y,t)$. Likewise the magnetic field is written as $B_z = B_{0z}(x) + \delta B_z(x,y)$. We also assume the quasi-neutrality condition $N_e = ZN_i$, where N_e and N_i are the electron and ion densities. The

equilibrium condition in this case is written as:

$$\kappa_B = \left(1+\frac{ZT_e}{T_i}\right)\frac{\beta_i}{2}\kappa_N + \frac{\beta_i}{V_{Ti}^2}g, \tag{2.1}$$

where:

$$\kappa_N = -\frac{1}{n_0}\frac{dn_0}{dx} > 0, \quad \kappa_B = \frac{1}{B_{0z}}\frac{dB_{0z}}{dx} > 0, \quad \beta_i = \frac{8\pi n_{0i}T_i}{B_0^2}.$$

As will be shown later, the characteristic wave numbers of the excited waves for the plasma parameters observed in the experiment (Fig. 2) are such that $k \leq \omega_{pi}/c$, where k is the wave number, ω_{pi} is the ion plasma frequency and c is the speed of light. For ion beta $\beta_i \sim 0.05$ this corresponds to values of $k\rho_i \ll 1$, where ρ_i is the ion Larmor radius. This means that hydrodynamic equations suitably modified to include magnetic viscosity can be used for the precursor plasma [16]. This was successfully demonstrated early on for the problem of flute mode instability of a plasma with a finite ion Larmor radius [17, 18]. Also, we should satisfy

$$\Omega_i\tau_i = 2x10^{11}BT_i^{3/2}/ZA^{1/2}\lambda n_i \ll 1$$

(τ_i is ion-ion collision time and λ is the Coulomb logarithm) and thus finite Larmor radius (FLR) effects are not pertinent. At the same time the total plasma beta $\beta = \beta_i + \beta_e \sim 0.5$.

It is also worth mentioning that the nonlinearity of low frequency flute modes is a rather coarse effect. The simplest and most natural way to describe this nonlinearity is thus within the framework of hydrodynamics. In the future we plan to carry out detailed investigations of the linear properties of electromagnetic flute modes using a kinetic approach.

The coupled nonlinear system of equations for density N, electrostatic potential Φ and magnetic field δB_z was derived in [1]. Below we present a system of equations modified in comparison with [1] where we retain nonlinear terms containing the perturbed magnetic field in equations for vorticity and electron density and also the perturbed magnetic field in the linear terms of the electron density equation. These equations can now be written in the following form:

$$\begin{aligned}
&\frac{\partial}{\partial t}\triangle_\perp\Phi + \frac{T_i c}{2ZeB_{0z}}\kappa_B\frac{\partial}{\partial y}\triangle_\perp\Phi + \frac{T_i}{Zen_{0i}}\frac{\partial}{\partial t}\triangle_\perp\delta n_i \\
&\quad - \frac{T_i}{2Ze}\frac{\partial}{\partial t}\triangle_\perp\frac{\delta B_z}{B_{0z}} + \frac{B_{0z}}{n_{0i}}\frac{g}{c}\frac{\partial\delta n_i}{\partial y} - \frac{g}{c}\frac{\partial\delta B_z}{\partial y} \\
&= \frac{cT_i}{2ZeB_{oz}}\{\Phi, \triangle_\perp(\frac{\delta B_z}{B_{0z}})\} - \frac{cT_i}{ZeB_{0z}n_{0i}}\nabla_\perp\{\Phi, \nabla_\perp\delta n_i\} - \frac{c}{B_{0z}}\{\Phi, \triangle_\perp\Phi\},
\end{aligned} \tag{2.2}$$

$$\begin{aligned}
&\frac{\partial\delta n_e}{\partial t} - \frac{cT_e}{eB_{0z}}\kappa_B\frac{\partial\delta n_e}{\partial y} + \frac{n_{0e}c}{B_{0z}}(\kappa_B+\kappa_N)\frac{\partial\Phi}{\partial y} - \frac{n_{0e}}{B_{0z}}\left(\frac{\partial\delta B_z}{\partial t} + \frac{cT_e}{eB_{0z}}\kappa_N\frac{\partial\delta B_z}{\partial y}\right) \\
&= \frac{c}{B_{0z}}\{\delta n_e, \Phi\} + \frac{cn_{0e}}{B_{0z}^2}\{\Phi, \delta B_z\}.
\end{aligned} \tag{2.3}$$

In (2.2) and (2.3) Poisson brackets are defined as:

$$\{a,b\}=\frac{\partial a}{\partial x}\frac{\partial b}{\partial y}-\frac{\partial a}{\partial y}\frac{\partial b}{\partial x},$$

and the $\perp$ subscript defines operations in the plane (x,y), perpendicular to an external magnetic field.

We will also use the following relation which connects δ_n and δB_z:

$$\frac{\delta B_z}{B_{0z}}=-\frac{1}{2}\beta\frac{\delta n}{n_0}, \tag{2.4}$$

where $\beta=\beta_i+\beta_e$.

Eqs. (2.2)-(2.4) describe the excitation and nonlinear evolution of compressible electromagnetic flute modes in a finite beta plasma with inhomogeneous magnetic field $B_{0z}(x)$. They will be used to analyze flute mode turbulence experimentally observed in the Z-pinch precursor region as well as in laboratory astrophysics experiments on interaction of laser ablated plasma flow with strong magnetic field created by the Zebra pulse power generator.

3 Linear theory analysis

The dispersion relation for flute mode instability can be obtained from the linearized equations (2.2)-(2.4). The dispersion relation was solved numerically for two different cases.

The first case is with plasma parameters typical of the Z-pinch experiments: $n_{0e}=2.0\times10^{19}cm^{-3}$, $n_{0i}=2.0\times10^{18}cm^{-3}$, $T_i\sim T_e=50eV$, $B_0=0.3MG$. The solution is displayed in Fig. 2, where the growth rates of the flute-like electromagnetic perturbations excited in the precursor region are plotted as a function of wave vector. As follows from Fig. 2, the flute modes can be excited in the wide range of wavelengths $0.1mm<\lambda<1mm$. The wavelengths of the excited waves are smaller then the radius of the precursor ($\sim1.5mm$) which satisfy the condition for the local approximation to hold, i.e., $\lambda<1.5mm$.

In the second case the dispersion relation was solved with the set of plasma parameters typical for experiments on interaction of laser ablated plasma flow with the strong magnetic field produced by the Zebra pulse power generator: $n_{0e}=1.0\times10^{18}cm^{-3}$, $n_{0i}=3.0\times10^{17}cm^{-3}$, $Ti\sim Te=150eV$, $B_0=(0.1-1.0)MG$ and $g\sim5^*10^{14}cm/s^2$. Only modes propagating along the plasma-magnetic field interface region (along the y-direction) were considered, because during the experiment only perturbations along the y-axis were observed. The solution of the dispersion relation is displayed in Fig. 3, where the frequency and growth rate of the flute-like electromagnetic perturbations are plotted as a function of wave vector ky. As follows from Fig. 3, for an external magnetic field $B_0=0.1MG$, the lowest possible wavelength of the excited flute modes along the y-direction is $\lambda\sim0.2mm$. The waves with wavelengths $0.2mm<\lambda<1.5mm$ can be excited in the system, because their

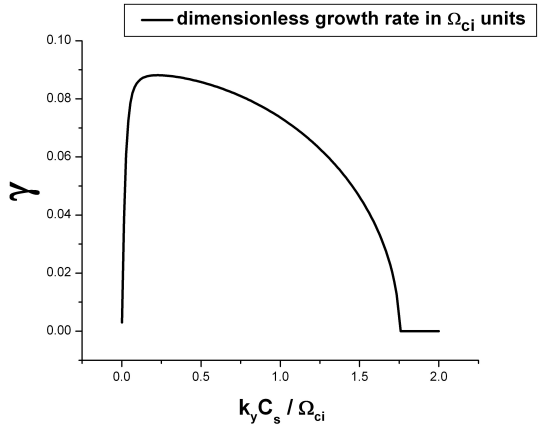

Figure 2: Dependence of the growth rate γ (in Ω_{ci} units) of the electromagnetic flute-type modes on the wave vector k_y (in units of the inverse Larmor radius defined through the electron temperature Ω_{ci}/C_s) for the experimental plasma parameters in the Z-pinch precursor.

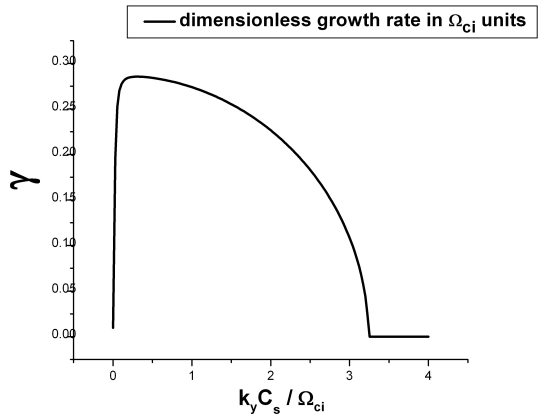

Figure 3: Dependence of the growth rate γ (in Ω_{ci} units) of the electromagnetic flute-type modes on the wave vector k_y (in units of the inverse Larmor radius defined through the electron temperature Ω_{ci}/C_s) for the experimental plasma parameters in laboratory astrophysics experiments.

wavelengths are smaller than the characteristic size of the laser ablated plasma plume in this direction. The growth rate yields a characteristic time for the instability to develop of $\sim 10ns$.

4 Numerical solution of nonlinear equations

In order to obtain numerical solutions of the nonlinear equations (2.2)-(2.4) we first rewrite them in dimensionless variables. For dimensionless time and space variables we will use

$$\tau = \Omega_{ci}t, \quad x = \frac{X}{c_s/\Omega_{ci}},$$

where $c_s^2 = T_e/M_i$. Dimensionless density and electrostatic potential are defined as:

$$\delta n = \frac{\delta n_i}{n_{0i}} = \frac{\delta n_e}{n_{0e}}, \quad \Phi = \frac{e\varphi}{T_e}.$$

We will also define the gravitational constant $g = 2c_s^2/R$ and $\rho_i^* = c_s/\Omega_{ci}$. Now, applying the Laplacian operator to both sides of Eq. (2.3) and eliminating the third term on the left hand side of Eq. (2.2), we are able to obtain the following system of nonlinear equations in dimensionless form:

$$\begin{aligned}\frac{\partial}{\partial\tau}\triangle_\perp\Phi - \frac{T_i}{T_e}\frac{V_n}{2+\beta}\frac{\kappa_B+(2+\frac{1}{2}\beta)\kappa_N}{\kappa_N}\frac{\partial}{\partial y}\triangle_\perp\Phi - \frac{1+\frac{1}{4}\beta}{1+\frac{1}{2}\beta}\frac{T_i}{T_e}V_n\frac{\frac{1}{2}\beta\kappa_N-\kappa_B}{\kappa_N}\frac{\partial}{\partial y}\triangle_\perp\delta n \\ +(1+\frac{1}{2}\beta)V_g\frac{\partial\delta n}{\partial y} = (1+\frac{1}{2}\beta)\frac{T_i}{T_e}div\{\nabla_\perp\Phi,\delta n\} - \frac{1}{4}\beta\frac{T_i}{T_e}\{\triangle_\perp\Phi,\delta n\} \\ +Z\{\triangle_\perp\Phi,\Phi\} + \mu\triangle_\perp(\triangle_\perp\Phi) - \frac{T_i}{T_e}(1+\frac{1}{4}\beta)D\triangle_\perp^2\delta n, \qquad (4.1)\end{aligned}$$

$$\frac{\partial\delta n}{\partial\tau} - \frac{ZV_n}{1+\frac{1}{2}\beta}\frac{\kappa_B-\frac{1}{2}\beta\kappa_N}{\kappa_N}\frac{\partial\delta n}{\partial y} + \frac{ZV_n}{1+\frac{1}{2}\beta}\frac{\kappa_B+\kappa_N}{\kappa_N}\frac{\partial\Phi}{\partial y} = Z\{\delta n,\Phi\} + D\triangle_\perp\delta n. \qquad (4.2)$$

In Eqs. (4.1)-(4.2), the viscosity μ and the coefficient of diffusion across the magnetic field D are such that:

$$\mu = \frac{3}{10}\frac{T_i v_i}{M_i\Omega_{ci}}, \quad D = \frac{m_e}{e^2}\frac{T_e v_e}{B_{0z}^2}. \qquad (4.3)$$

In order to numerically solve the nonlinear system of equations (4.1)-(4.2) the two-dimensional code FLUTE has been developed. In this code a two-step time integration scheme was used. Taking the density equation as an example we show below the predictor step (from time step n to $n+1/2$):

$$n_p^{n+1/2} = <n>^n + \frac{\triangle t}{2}F_n^n + \frac{\triangle t}{2}D_n(\nabla_\perp^2 n)^n, \qquad (4.4)$$

with optional Lax spatial average:

$$<n> = \frac{1}{4}(n_{i+i,j}+n_{i-1,j}+n_{i,j+1}+n_{i,j-1}). \qquad (4.5)$$

Otherwise:

$$<n> = n_{i,j}. \qquad (4.6)$$

The corrector step (from time step n to $n+1$) is such that:

$$n_c^{n+1} = n^n + \triangle t F_{n_p}^{n+1/2} + \triangle t D_n(\nabla_\perp^2 n)^n, \qquad (4.7)$$

where F_n is given by:

$$F_n = -C_n^1\frac{\partial n}{\partial y} - C_n^2\frac{\partial\phi}{\partial y} + C_n^3\{n,\phi\}, \qquad (4.8)$$

and C_n^1, C_n^2 and C_n^3 regroup the appropriate coefficients in Eq. (4.2). In the code diffusivity and viscosity were treated explicitly in time. We also use space-centered derivatives:

$$\frac{\partial n}{\partial y}=\frac{(n_{i,j+1}-n_{i,j-1})}{2\triangle y}. \tag{4.9}$$

The nonlinear advective terms in Poisson brackets such as:

$$\{n,\phi\}=\frac{\partial n}{\partial x}\frac{\partial \phi}{\partial y}-\frac{\partial n}{\partial y}\frac{\partial \phi}{\partial x}=J(n,\Phi), \tag{4.10}$$

were handled using Arakawa's conservative method [19,20]:

$$\begin{aligned}J_{i,j}(n,\phi)=&-\frac{1}{12\triangle x\triangle y}[(\phi_{i,j-1}+\phi_{i+1,j-1}-\phi_{i,j+1}-\phi_{i+1,j+1})(n_{i+1,j}-n_{i,j})\\&+(\phi_{i-1,j-1}+\phi_{i,j-1}-\phi_{i-1,j+1}-\phi_{i,j+1})(n_{i,j}-n_{i-1,j})\\&+(\phi_{i+1,j}+\phi_{i+1,j+1}-\phi_{i-1,j}-\phi_{i-1,j+1})(n_{i,j+1}-n_{i,j})\\&+(\phi_{i+1,j-1}+\phi_{i+1,j}-\phi_{i-1,j-1}-\phi_{i-1,j})(n_{i,j}-n_{i,j-1})\\&+(\phi_{i+1,j}+\phi_{i,j+1})(n_{i+1,j+1}-n_{i,j})+(\phi_{i,j-1}-\phi_{i-1,j})(n_{i,j}-n_{i-1,j-1})\\&+(\phi_{i,j+1}-\phi_{i-1,j})(n_{i-1,j+1}-n_{i,j})+(\phi_{i+1,j}-\phi_{i,j-1})(n_{i,j}-n_{i+1,j-1})].\end{aligned} \tag{4.11}$$

The fourth order derivative of density in the dissipative term of the vorticity equation has been treated as a biharmonic operator [21]:

$$\begin{aligned}\nabla^4 n_{i,j}=&\frac{1}{(\triangle x)^2(\triangle y)^2}\Big[20n_{i,j}-8(n_{i+1,j}+n_{i,j+1}+n_{i-1,j}+n_{i,j-1})\\&+2(n_{i+1,j+1}+n_{i+1,j-1}+n_{i-1,j+1}+n_{i-1,j-1})+(n_{i,j+2}+n_{i+2,j}+n_{i-2,j}+n_{i,j-2})\Big].\end{aligned} \tag{4.12}$$

The potential is obtained from the vorticity using Fast Fourier Transforms (FFT2 or FFTW):

$$\phi_k=-\frac{1}{k^2}U_k. \tag{4.13}$$

An additional and important feature of the numerics is the dynamic time step. Initially the nonlinear numerical calculations are started with a suitably small and numerically stable normalized time step $dt_0=0.05$. The maximum velocity in all directions on the grid v_{max} is continuously monitored during the calculations and the time step is adjusted dynamically to $dt-dy_n=0.5/v_{max}$ when $dt-dy_n<dt_0$. This insures that all perturbations on the grid are temporally well resolved throughout the calculations.

In Fig. 4 the time evolution and saturation of the square of absolute value of electrostatic potential $|\Phi|^2$ and density perturbations $|\delta n|^2$ are presented. After a period of exponential growth with the linear growth rate of electromagnetic flute modes, the instability saturates due to nonlinear mode interactions (through the nonlinear terms in Poisson brackets in Eqs. (4.1) and (4.2) and the presence of viscous and diffusion terms.

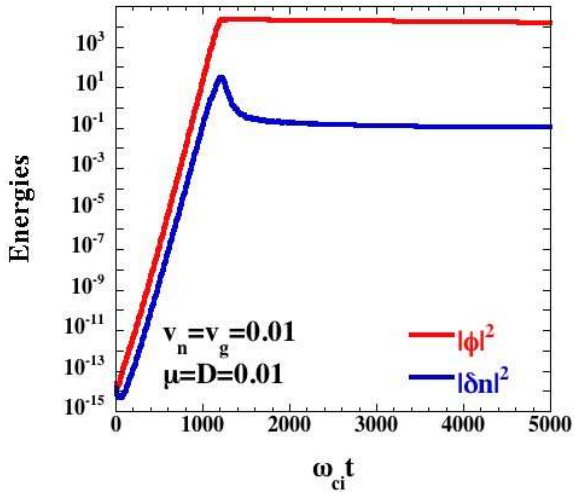

Figure 4: Evolution in time of the sum over all Fourier harmonics of $|\Phi|^2$ and $|\delta|^2$ obtained from numerical solutions of Eqs. (4.1)-(4.2).

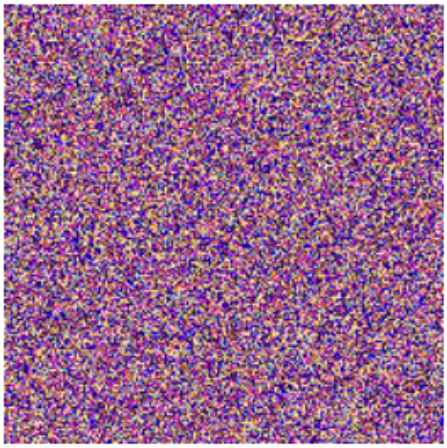

Figure 5: Random initial density perturbations with $\delta n/n_0 \sim 10^{-6}$.

In the series of figures below the evolution in time of initially randomly seeded density perturbations is presented. The initial level of density perturbations presented in Fig. 5 is $\delta n/n_0 \sim 10^{-6}$.

In Fig. 6 density perturbations in the linear stage of flute mode instability development are presented. It is clearly seen that perturbations are elongated along the x-axis. This is directly connected with the fact that the growth rate is largest for waves propagating along the y-axis and for such waves $k_x \ll k_y$. This results in a much shorter scale for perturbations in the y-direction.

In Fig. 7 the density perturbations in the nonlinear stage of flute mode instability

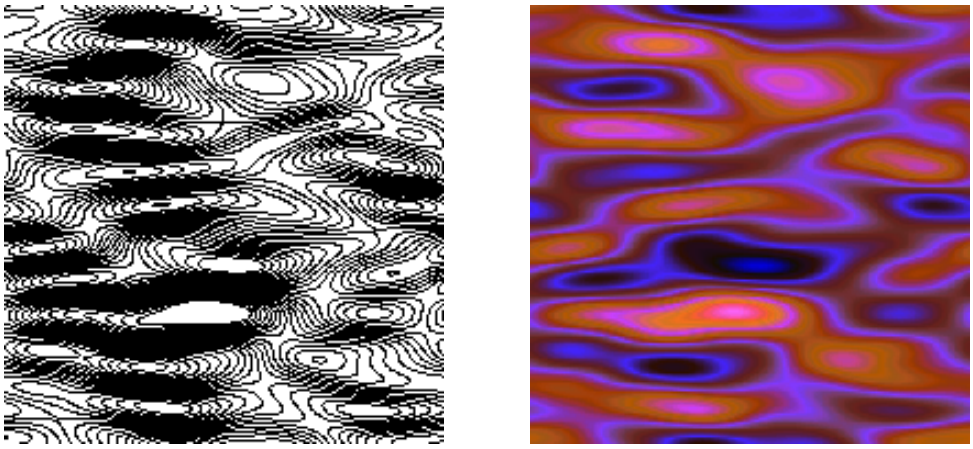

Figure 6: Growth of density perturbations in the linear stage of flute mode instability in (x,y) plane. The left and right plots correspond to the same data but the right plot in black and white has higher pictorial resolution.

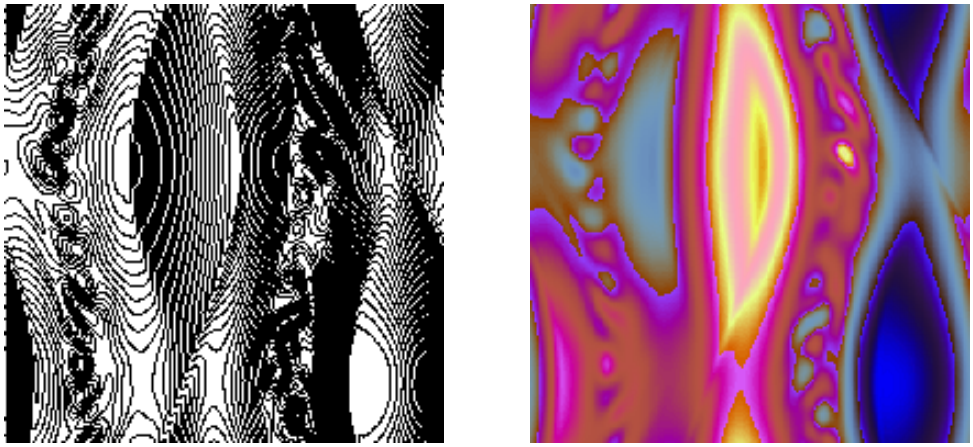

Figure 7: Formation of large scale structures and short scale perturbations in the nonlinear stage of flute mode instability in (x,y) plane. The left and right plots correspond to the same data but the right plot in black and white has higher pictorial resolution.

are presented. One can observe formation of large scale structures and on top of them development of short scale perturbations. The appearance of modes with $k_x \sim k_y$ in this stage is due to nonlinear interaction between the unstable flute modes.

5 Experimental results

In the early stages of wire array implosion part of the current flows through the plasma column of the Z-pinch precursor which forms as ablated material reaches the axis. Multiframe shadowgraphy has revealed the appearance of strong wave turbulence in the

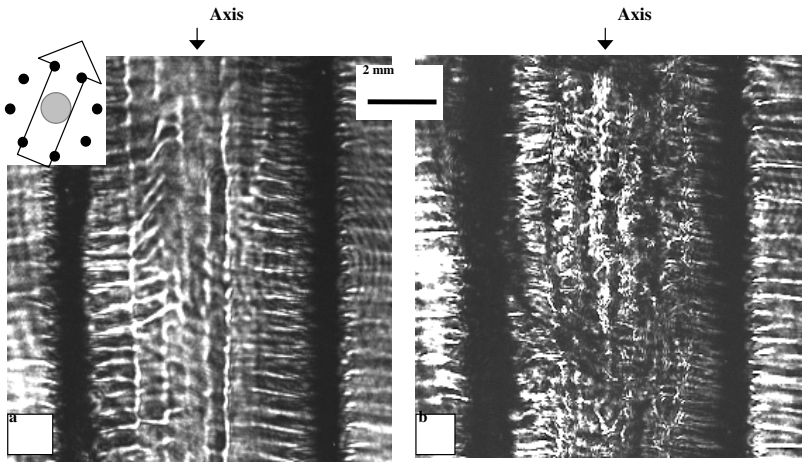

Figure 8: Development of plasma turbulence in the precursor of the $Al \quad 8\times 15\mu m$ wire array. Shadowgrams of the precursor plasma at instants with 20 ns separation in time. In (a) - seeded density perturbations are presented. In (b) - at late times formation of large and short scales is observed.

precursor stage in the central plasma column of the Al wire array. A detailed description of experimental results can be found in [1, 2, 22]. The latest experimental result obtained with multiframe shadowgraphy and presented in Fig. 8 also demonstrates formation in late times of large and short scales in the perturbed density initially seeded with perturbations of typical size $\sim 0.5mm$.

Another application, with similar linear and nonlinear consequences, of the model of compressible electromagnetic flute mode instability is connected with laboratory experiments on interaction of laser ablated plasma flow with magnetic field [4] where flute mode instability can develop in the region of plasma flow deceleration by the magnetic field. In this experiment [4] a plasma flow was produced by laser ablation and was decelerated by the external magnetic field produced by the Zebra pulse power generator. The interaction region was diagnosed with multiframe schlieren imaging. About 5 ns after the creation of the plasma, the plasma-field boundary became unstable, with perturbations growing in the plane perpendicular to the magnetic field, but not in the plane containing the magnetic field lines. Fourier analysis showed a dominant wavelength of about $0.5mm$, close to the maximum growth rate predicted for the experimental conditions (see Fig. 3). At 7 ns later one can notice cascading in the spectrum towards both shorter and longer wavelengths. These experimental results are indeed similar to the previous ones in Z-pinch precursor plasmas.

6 Discussion and conclusions

The instability of compressible electromagnetic magnetic-curvature-driven flute-like modes in a finite-beta plasma has been investigated to explain the experimentally ob-

served excitation of turbulence in the precursor plasma of imploding wire arrays in Z-pinches and in laser ablated plasma flows during their interaction with the strong magnetic field produced by the Zebra pulse power generator.

In a low beta plasma flute modes are electrostatic oscillations propagating in the plane perpendicular to the external magnetic field. In both the finite beta precursor plasma and in the laser ablated plasma flow interacting with the magnetic field, it is necessary to treat the flute modes as electromagnetic. The presence of the electromagnetic component in the wave field leads to significant changes in the dispersion relation of the flute modes. Inclusion of finite plasma beta effects also results in the appearance of new nonlinear terms. Nevertheless this does not prevent the emergence of the instability of the flute modes and the formation of large and small scale perturbations in the system.

The experimentally observed spatial and temporal scales of large-scale cells and small-scale density perturbations correspond to those predicted by our theoretical model of compressible electromagnetic flute mode turbulence.

In the future we plan to investigate the appearance in such systems of zonal modes and streamers and their interaction with the isotropic flute modes.

Acknowledgments

This work was supported by the United States Department of Energy under the following grants: Grant No. DE-FC52-01NV14050 at the University of Nevada at Reno, Grant No. DE-AC04-94AL85000 at Sandia National Laboratories. Sandia is a multiprogram laboratory operated by Sandia Corporation, a Lockheed Martin Company, for the U.S. DOE under Contract DE-AC04-94AL85000.

References

[1] V.I. Sotnikov, V.V. Ivanov, T.E. Cowan, J.N. Leboeuf, B.V. Oliver, C. Coverdale, B. Jones, C. Deeney, T. A. Mehlhorn, G. S. Sarkisov and P.D. LePell, Investigation of Electromagnetic Flute Mode Instability in a High Beta Z-pinch Plasma, IEEE Transactions in Plasma Sci., 34 (2006), 5-10.

[2] V. Ivanov, G.S. Sarkisov, P.J. Laca, V.I. Sotnikov, V.L. Kantsyrev, et al., Investigation of magnetic fields in 1-MA wire arrays and X-pinches, IEEE Transactions in Plasma Sci., 34 (2006), 10-15.

[3] V.I. Sotnikov, R. Presura, V.V. Ivanov, T.E. Cowan, J.N. Leboeuf and B.V. Oliver, Excitation of electromagnetic flute modes in the process of interaction of plasma flow with inhomogeneous magnetic field, Astrophysics and Space Physics, 307 (2007), 99-101.

[4] R. Presura, V. Ivanov, Y. Sentoku, V. Sotnikov, N. Le Galloudec, A. Kemp, R. Mancini, H. Ruhl, A. Astanovitskiy, P. Laca, T. Cowan, T. Ditmire, C. Chiu, W. Horton, P. Valanju and S. Keely,Laboratory simulation of magnetospheric plasma shocks, Astrophysics and Space Science, 298 (2005), 299-304.

[5] Y.P. Zakharov, Collisionless laboratory astrophysics with lasers, IEEE Transactions in Plasma Sci., 31 (2003), 1243-1251.

[6] V.P. Lakhin, S.V. Makurin, A.B. Mikhailovskii and O.G. Onishchenko, Dispersion ion- drift hydrodynamics, J. Plasma Phys., 38 (1987), 387-405.
[7] P.A. Bernhardt, R. A. Roussel-Dupre, M. B. Pongratz, G. Haerendel, A. Valenzuela, D. A. Gurnett, R. R. Anderson, et al., Observations and theory of the AMPTE magnetotail barium releases, J. Geophys. Res. A 92 (1992), 5777-5794.
[8] B.H. Ripin, J.D. Huba, E.A. McLean, C.K. Manka, T. Peyser, H. R. Burris and J. Grun, Sub-Alfvénic plasma expansion, Phys. Fluids B 5 (1993), 3491-3499.
[9] R. Z. Sagdeev, V. D. Shapiro and V. I. Shevchenko, Convective cells and anomalous plasma diffusion, Sov. J. Plasma Phys., 4 (1979), 306-314.
[10] W. Horton, Drift waves and transport, Rev. Mod. Phys., 71 (1999), 735-778.
[11] D. E. Newman, P. W. Terry, P. H. Diamond and Y. M. Liang, The dynamics of spectral transfer in a model of drift wave turbulence with two nonlinearities, Phys. Fluids B, 5 (1993), 1140-1153.
[12] P. Beyer, S. Benkadda, X. Garbet and P. H. Diamond, Nondiffusive transport in tokamaks: Three-dimensional structure of bursts and the role of zonal flows, Phys. Rev. Lett., 85 (2000), 4892-4896.
[13] V. P. Pavlenko and V. I. Petviashvili, Solitary vortex in a flute instability, Sov. J. Plasma Phys., 9 (1983), 603-604.
[14] Z. N. Andrushchenko and V. P. Pavlenko, Turbulent generation of large-scale flows and nonlinear dynamics of flute modes, Phys. Plasmas, 9 (2002), 4512-4519.
[15] I. Sandberg and P. K. Shukla, Magnetic-curvature-driven interchange modes in dusty plasmas, Phys. Plasmas, 11 (2004), 542-547.
[16] I. Sandberg, Z. N. Andrushchenko and V. P. Pavlenko, Large-scale flows and coherent structure phenomena in flute turbulence, Phys. Plasmas, 12 (2005), 042311-1042311.
[17] A. B. Mikhailovskii, Theory of plasma instabilities. New York: Consultants Bureau, 1974.
[18] K. V. Roberts and J. B. Taylor, Magnetohydrodynamic equations for finite Larmor radius, Phys. Rev. Lett., 8 (1962), 1972001.
[19] A. Arakawa, J. Comput. Phys., 1 (1966), 119-143. Reprinted as A. Arakawa, Computational design for long-term numerical integration of the equations of fluid motion: two-dimensional incompressible flow, J. Comput. Phys., 135 (1997), 103-114.
[20] D. Brock and W. Horton, Toroidal drift-wave fluctuations driven by ion pressure gradients, Plasma Phys., 24, 271-287 (1982).
[21] M. Abramowitz and I.A. Stegun, Handbook of Mathematical Functions, Dover Publications, Inc., New York, 1972.
[22] V. Ivanov, V. V. Ivanov, V. I. Sotnikov, T. E. Cowan, P. J. Laca, A. L. Astanovitskiy, B. Le Galloudec, G. S. Sarkisov, B. Jones, C. Deeney, B. V. Oliver, T. A. Mehlhorn and J. N. Leboeuf, Experimental study of dynamics of large- and small-scale structures in the plasma column of wire array Z-pinches, IEEE Transactions in Plasma Sci., 35 (2007), 10-15.